Lanthanum Oxide Doped Calcium Silicates Particles: Preparation and Characterization

İsmail Seçkin ÇARDAKLI[1]*

[1]Atatürk Üniversitesi, Mühendislik Fakültesi, Metalurji ve Malzeme Mühendisliği Bölümü, 25240, Erzurum, Türkiye

Abstract: Bioactive calcium silicate (CS) and lanthanum oxide (La_2O_3) doped bioactive calcium silicate (La-CS) materials were successfully prepared in this study. CaO, SiO_2, and La_2O_3 used as precursors materials followed by the solid-state reaction at 1050°C for 2h. The retained particles were crushed and characterized using various methods such as XRD, FTIR, and SEM. Based on the XRD analysis outcomes, two phases of calcium silicate ($CaSiO_3$ and Ca_2SiO_4) were obtained, and the quantity of $CaSiO_3$ phase increased gradually with increasing La_2O_3 amount. Based on the FTIR analysis outcomes, the sharpness and area of SiO_4 group shrinkage with the addition of La_2O_3. Based on the SEM analysis outcomes, calcium silicate particles appeared as spheroids like particles and transformed to elongated spheroidal particles with the addition of 20 wt.% of La_2O_3. Furthermore, incorporating 20 wt.% of La_2O_3 reduced the size of calcium silicate particle up to 60% of the pure samples.

Lantanyum Oksit Katkılı Kalsiyum Silikat Partikülleri: Hazırlanışı ve Karakterizasyonu

Özet: Bu çalışmada, biyoaktif kalsiyum silikat (CS) ve lantan oksit (La_2O_3) katkılı biyoaktif kalsiyum silikat (La-CS) malzemeleri başarıyla hazırlanmıştır. Öncü malzemeler olarak CaO, SiO2 ve La_2O_3 kullanıldı ve ardından 2 saat boyunca 1050 °C'de katı hal reaksiyonu gerçekleştirildi. Parçacıklar ezildi ve X-ışını kırınım analizi (XRD), Fourier kızılötesi spektroskopisi (FTIR) ve Taramalı elektron mikroskobu (SEM) gibi çeşitli yöntemler kullanılarak karakterize edildi. XRD analizi sonuçlarına göre kalsiyum silikat iki fazı ($CaSiO_3$ ve Ca_2SiO_4) elde edildi ve artan La_2O_3 miktarı ile $CaSiO_3$ fazı miktarı kademeli olarak arttı. FTIR analizinin sonuçlarına göre, La_2O_3 ilavesiyle SiO_4 grubu büzülmesinin keskinliği ve alanı arttı. SEM analizinin sonuçlarına göre, kalsiyum silikat partikülleri küresel olarak göründü ve ağırlıkça %20 La_2O_3 ilavesiyle uzatılmış küresel partiküllere dönüştü. Ayrıca, La_2O_3'ün ağırlıkça %20'sinin dahil edilmesiyle kalsiyum silikat partikül boyutu saf numunelerin partikül boyutunun %60'ına kadar azaldı.

1. Introduction

The bioactive and biocompatible materials have extensively been studied and employed to repair, reconstruct, and replace damaged living hard tissues or worsen body parts, particularly badly accidental bones, and teeth. Mostly the used materials involved glass-based silicate ceramic materials due to their ability to slight and slow but gradual solubility in the living body fluid. These silicate glass-ceramic materials can be long-term implanting materials due to their bioactive nature. This bioactive behaviour further results from their ability to develop a good and strong binding behaviour with the living hard tissues. Additionally, a biologically active carbonated apatite layer appears on the bioactive materials that further bonding the surface with the bone tissues. In this connection, silicon-based substances play a major role in enriching the bioactive capability of glass-based materials [1]. Hench introduced the first bioactive glass bioglass in 1971, which is still the most popular clinical material for various biomedical applications [2]. Since the Hench discovery, various biomaterials, particularly calcium silicate [Wollastonite ($CaSiO_3$)] and bioactive glass-based materials, gained huge popularity as highly promised biomaterials for orthopaedic surgery [3]. Silicon is an important trace element and has shown an encouraging function in the early growth of bones. Its soluble form may play a pivotal role in the production and osteoblastic

differentiation in human osteoblast cells and the stimulation of collagen cells [4]. According to the previous studies, it has been exhibited that $CaSiO_3$ based materials have revealed excellent bioactivity and biocompatibility and have a strong capability to connect with the living hard tissues. These investigations demonstrated that $CaSiO_3$ oriented bioglass might prove significant and trustable material for different orthopaedic related surgical problems. Since $CaSiO_3$ ceramic materials have shown significantly in vitro bioactivity and biocompatibility [5], owing to these potential properties, $CaSiO_3$ have been studied extensively to use them as artificial bones and dental roots. Since then, $CaSiO_3$ has gained an escalating attraction in the clinical area, especially in the orthopedic surgery and drug delivery. This huge attention and attraction have been attributed to the greater ability of $CaSiO_3$ to develop good bioactivity, biocompatibility and sealing capability [6, 7].

Compositional doping in $CaSiO_3$ by various ions like titanium, magnesium, europium etc., has already been reported in the literature, which successfully showed an improvement in the biological and physicochemical properties of $CaSiO_3$. However, a major drawback of $CaSiO_3$ is its high dissolution rate after its implantation, which may be fatal for the surrounding tissues. Therefore, there is a need to improve its characteristics to improve its properties for various biomedical applications, particularly after its implantation in the living environment.

In this regard, the addition of titanium, magnesium, strontium etc. Lanthanum and lanthanum Oxide (La_2O_3) are novel materials with many industrial, technological, and biomedical applications. Lanthanum ion has been known due to its antibacterial role. Its substitution in the $CaSiO_3$ may help enhance its role in controlling different bacterial infections, inflammation, and bone tissue resorption [8, 9]. Numerous previous studies have revealed that lanthanum and silicon substituted biomaterials have applications in the biomedical area [10, 11]. Similarly, according to some reports, La_2O_3 also has been found an attractive material to improve the mechanical and biological properties of the materials in which they are substituted [12]. Besides this, the literature also reported that the use of lanthanum helps in controlling the inordinate number of calcium effects in the biological system.

Moreover, lanthanum and facilitates in blocking lanthanum use and facilitates the blocking of active calcium extraction in the human red blood cells [13]. Furthermore, lanthanum has been reported to have good mechanical strength, powerful antibacterial property, anti-inflammatory effect, rapid wound healing effect, biocompatibility, bioactivity, and helps in restoring skin tissues and functions when used in the biological system [14-16]. Therefore, it is commonly a developed analogy that incorporating

lanthanum in the $CaSiO_3$ may be beneficial in uplifting the characteristics of the $CaSiO_3$ materials [14, 17].

Various techniques are constantly in use to synthesize these bioceramic materials. Precipitation, hydrothermal, co-precipitation, sol-gel, microwave-assisted methods, and continuous flow microwave are the well-known routes to prepare these biomedical materials [18-21]. These are the liquid phase-based methods that have many merits over solid-state methods. Still, their long processing time and maintenance of various process parameters make them a difficult choice. Owing to these demerits' scientists are trying to use solid-state methods that involve fewer process parameters and short process time [22].

The aim of this study was to synthesis and characterize calcium silicate and La doped calcium silicate materials, and to evaluate the impact of dopant (La_2O_3) on physiochemical properties of calcium silicate. The objectives of this study were achieved, and the results discussed in detail in the results section. In literature, La_2O_3 incorporation into the calcium silicate lattice and its impact on the crystal structure has not been reported. Therefore, in this study, the effect of La_2O_3 substitution on the crystal structure, particle shape and particle size of calcium silicate is reported for the first time.

2. Material and Method

Calcium carbonate ($CaCO_3$, Merck), Silicon dioxide (SiO_2, Merck), and Lanthanum (III) oxide (La_2O_3. Merck) were used as precursors materials.

2.1 Preparations of $CaSiO_3$ and La-doped $CaSiO_3$

The entire materials were synthesised using the Solid-state method. Briefly, 1 M (10 g) of $CaCO_3$ powder was mixed thoroughly with 1 M (6 g) of SiO_2 using mortar and pestle for about 10 mint. Then, the powder mixture transferred to the furnace and heat-treated at 1050ºC for 2 h (Solid-state method). For La-doped $CaSiO_3$, the molar ratio of (Ca+La)/Si was fixed to 1. Different amounts of La_2O_3 powder were mixed with $CaCO_3$ powder before mixing it with SiO_2. The concentration of chemical utilized to synthesis pure $CaSiO_3$ and La-doped $CaSiO_3$ materials were recorded in Table 1.

Table 1. Quantities of the reactants.

Sample ID	Reactants (Mole%)		
	CaO	La_2O_3	SiO_2
CS	50 %	00	50 %
10% La-CS	40 %	10%	50 %
20% La-CS	30 %	20%	50 %

A graphic illustration of the preparation of pure $CaSiO_3$ and La-doped $CaSiO_3$ materials is displayed in Figure. 1.
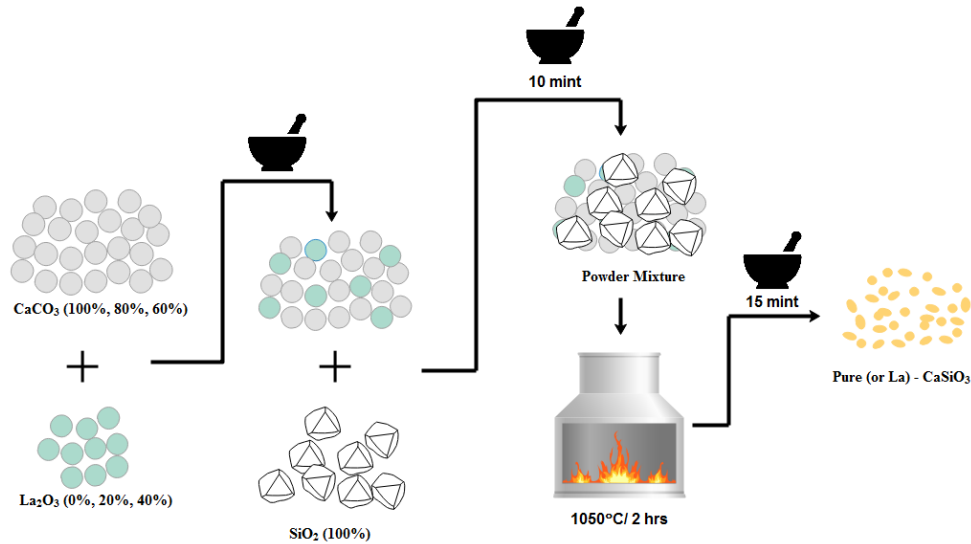
Figure 1. A schematic illustration of the preparation of materials

2.2 Characterizations

The calcined powder was crushed using mortar and pestle. The phase purity of the prepared materials was examined by X-ray diffraction analysis (XRD, Bruker) in the 2θ range of 5°–90° (step size 0.03/sec). The quantitative determination of the crystalline phases was calculated with integrated software. The particles shape and elemental distribution of the materials were investigated by scanning electron microscopy (SEM, ZEISS). Random points on the SEM image have been selected to assess the particle size distribution using image analysis software ImageJ. The functional groups that existed in the prepared materials were determined using Fourier Transform Infra-Red Spectrometer (FTIR, Bruker) in the range of 400-4000 cm^{-1}.

3. Results

3.1. X-ray diffraction

Calcium silicate is well known biocompatible material and has promising as a future material in bone tissue applications. It has been successfully synthesised using different techniques such as sol-gel method [24], wet precipitation method [25], hydrothermal synthesis method [26], mechanochemical-assisted solid-state [23], water vapour-assisted solid-state [27], solid-solid fusion method [28], and molten salt method [28]. In this study, we have used the solid-state method to synthesis calcium silicate (CaSiO$_3$) and La-doped CaSiO$_3$. The XRD technique has been used to examine the purity and quantity of the obtained phases, and the results illustrated in Figure 2 and Table 2. Here, we have used calcite (CaCO$_3$) as a source of CaO, which later used as the main ingredient of calcium silicate. Widayat et al. demonstrated that heat-treated CaCO$_3$ at ≥900ºC decomposed to CaO [29]. Atchudan et al. obtained spherical CaO nanoparticles at ≥650ºC [30]. Furthermore, Yamashita et al. demonstrated that CaCO$_3$ fully decomposed to

form CaO at 700°C [31]. Our results were in the same trend with previous studies, no traces for calcite has been observed in all the samples, as shown in Fig 2. X-ray diffraction analysis of mixed CaO and SiO$_2$ at 1:1 molar ratio calcined at 1050°C for 2h shown in Fig. 2(a). It is observed that after the calcination process, the diffraction planes of the final materials were in the crystalline phase. The calcite phase no longer existed, deduced that it had completely transformed to CaO. The calcium silicate existed in multiple phases, such as calcium silicates (CaSiO$_3$) (38.9%) and dicalcium silicates (Ca$_2$SiO$_4$) (2.8%), as shown in the Equations (1-3) [32].

$$CaCO_3 \rightarrow CaO + CO_2 \qquad (1)$$

$$CaO + SiO_2 \rightarrow CaSiO_3 \qquad (2)$$

$$2CaO + SiO_2 \rightarrow Ca_2SiO_4 \qquad (3)$$
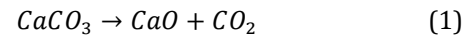
CaO was still detected in all the samples. This is because CaO has a high melting temperature of around 2572 ºC or could be attributed to poor fusion of CaO with SiO$_2$ to form calcium silicate.

With the addition of La$_2$O$_3$, some diffraction planes correlated to La$_2$O$_3$ were presented (Fig 2(b, c), which confirmed that some amount of La$_2$O$_3$ deposited on the surface of calcium silicates rather than substituted into lattice crystal. However, it can be seen that the amount of CaSiO$_3$ phase was increased with an addition of La$_2$O$_3$ compared to pure CS samples (Table 2). This behaviour could be due to the presence of La$_2$O$_3$, which acted as a flux material and further lowered the melting point of CaO.

Table 2. The phase averaged quantities exhibited in CS and La-doped CS materials

Sample ID	Phase Quantity (%)				
	CaO	SiO$_2$	La$_2$O$_3$	CaSiO$_3$	Ca$_2$SiO$_4$
CS	54.3	4.0	0	38.9	2.8
10% La-CS	3.9	0.2	6.5	30.5	58.9
20% La-CS	4.1	0.4	17.2	72.5	5.8
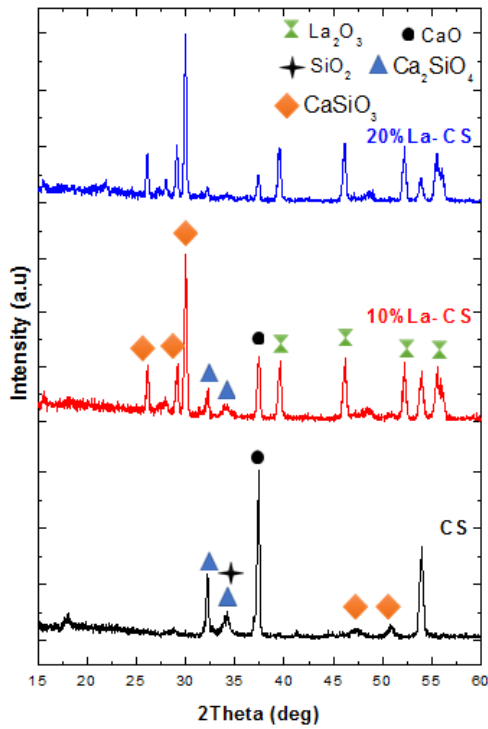
Figure 2. XRD pattern of the pure CS and La-doped CS materials calcined at 1050 ºC for 2 h.

3.2. FTIR analysis

The FTIR spectra of pure CS and La-doped CS calcined at 1050ºC were shown in Figure 3. In the spectra, the major bands related to the silicate groups are attributed to the SiO_4^{4-} tetrahedral have appeared. The band located in the range of 800-900cm^{-1} was appointed to the stretching mode of Si-O (υ1) and the antisymmetric stretching of Si–O–Si (υ2) was exhibited as a broadband in the range of 800-1000cm^{-1}. Furthermore, the bending mode of Si-O (υ3 and υ4) should be detected at 300-350 cm^{-1} and 400-500 cm^{-1}, respectively.
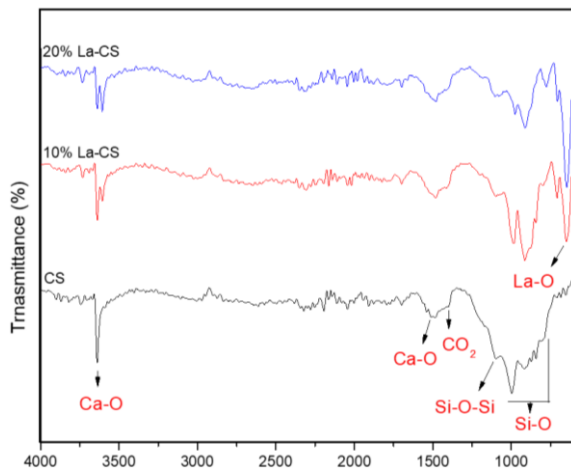
Figure 3. FTIR spectra of the pure CS and La-doped CS materials calcined at 1050 ºC for 2 h

These results are in good match with the previous research conducted by Bouregba et al. and Puertaset et al. [33, 34]. The standard stretching vibration of the

C=O group was detected at 1387 cm^{-1}, the CO_2 formed as side product due to decomposition of $CaCO_3$ to CaO, as illustrated in the Eq. 1(a) [35]. The absorption bands noted around 3637 and 1506 cm^{-1} are the characteristic absorption bands of CaO [34]. After modifying the pure CS with La_2O_3, one absorption peak attributed to La-O bond appeared at nearly 645 cm^{-1}. Consequently, the presence of the above-stated bands recognizes the existence of La_2O_3 [36]. The sharpness and area of SiO_4 group shrinkage with the addition of La_2O_3 which could be ascribed to the difference of electronegativity and polarizing power between La^{3+} and Ca^{2+} [37]. Furthermore, the peaks of SiO_4 group shifted to low value of wavenumber which could be attributed to crystal structure disorder of CS or confirming partial substitution of lanthanum ions into the CS lattice [37].

3.3. Microstructure and particle distribution analysis

Microstructure analysis and particle distribution of the pure CS and La-doped CS materials calcined at 1050 ºC for 2 h were displayed in Figure 4-5. As seen in Fig. 4(a), pure CS particles consisted of densely packed particles and appeared as spheroid-like particles with diameter size in the range of 230-510 nm. Furthermore, spherical materials have the benefit that they have no threat for irritation or destruction of mucosal layers [38].
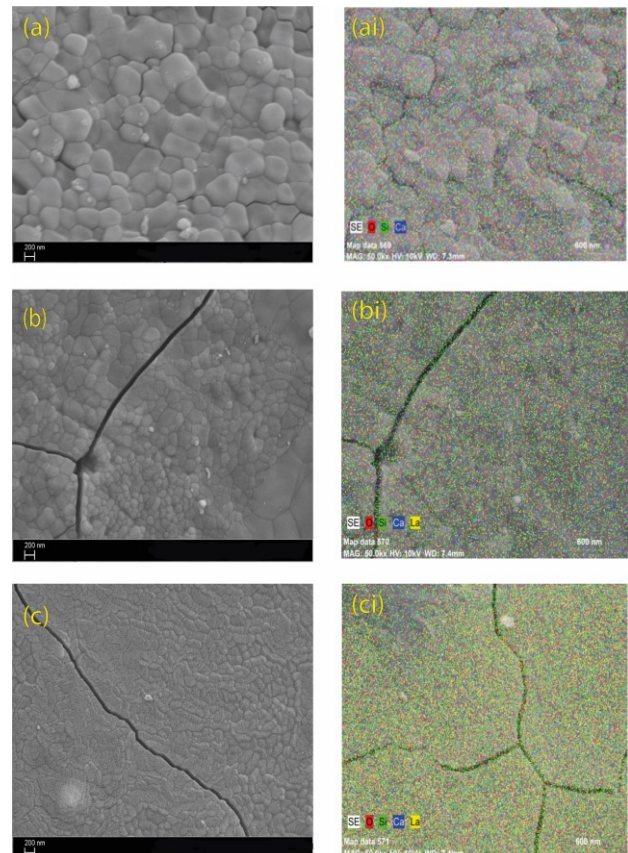
Figure 4. (a, ai) SEM image and elemental mapping of pure CS, (b, bi) SEM image and elemental mapping of 10%La-CS, and (c, ci) SEM image and elemental mapping of 20%La-CS materials calcined at 1050ºC for 2 h.

With the addition of 10 wt. % of La_2O_3, no obvious effect has been observed in the shape of the particles. Research performed by Jadalannagari et al. observed that the incorporation of La^{3+} ions did not significantly affect the morphology of the hydroxyapatite (HA) particles [39]. However, the particle size was significantly decreased to the range of 102-211nm. By increasing the La_2O_3 amount to 20 wt.%, the particles size decreased to the range of 97-195 nm. Bozkurt et al demonstrated that the grain size of commercially synthetic HA powders decreases by increasing La_2O_3 amount [40]. This behaviour could be correlated to the different valence of La^{3+} and Ca^{2+}, La^{3+} substituted part of Ca^{2+} in the calcium silicates crystal lattice, was able of suppressing the size growth of calcium silicate particles [41]. Furthermore, the morphology of CS particles has been also affected by an increasing amount of La_2O_3, and the particle shaped changed from spheroid -like particles for pure CS to elongated spheroidal particles for 20%La-CS. Furthermore, successful homogenous incorporation of La_2O_3 into the calcium silicate structure was further verified via the elemental mapping of Ca, Si and La elements by using SEM (Figure 4. (ai,bi,ci).
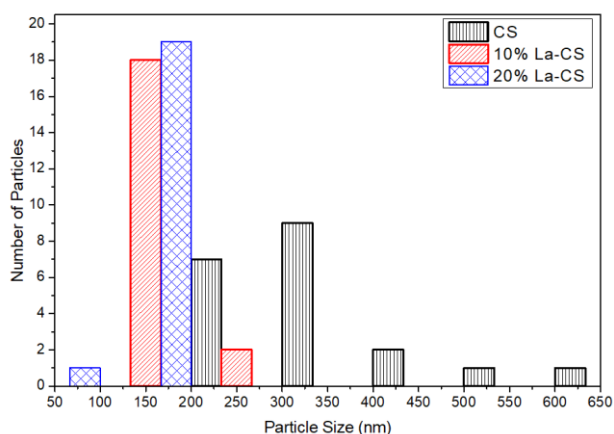
Figure 5. Particle size distribution histogram of the prepared materials.

4. Discussion and Conclusion

In the summary, multiphase of pure and doped calcium silicate were successfully prepared using a solid-state method. The amount of wollastonite ($CaSiO_3$) increased gradually upon the increasing amount of La_2O_3 in the structure of the material. Significant shrinkage in the particle size of calcium silicate with the addition of La_2O_3 has been observed. Substitution higher amount of La_2O_3 (20 wt.%) changed the particle shape from spheroids to elongated spheroidal particles. The bending and stretching vibrations mode of silicate, CaO, and La_2O_3 were observed. Finally, a new kind of bioceramics have been prepared and characterised in this study, and it can be used as a potential candidate for cell culture analysis.

Declaration of Ethical Code

In this study, we undertake that all the rules required to be followed within the scope of the "Higher Education Institutions Scientific Research and Publication Ethics Directive" are complied with, and that none of the actions stated under the heading "Actions Against Scientific Research and Publication Ethics" are not carried out.

References

[1] T. Kokubo. 1990.Surface chemistry of bioactive glass-ceramics, Journal of Non-Crystalline Solids, 120(1-3), 138-151.

[2] L.L. Hench, R.J. Splinter, W. Allen, T. Greenlee. 1971. Bonding mechanisms at the interface of ceramic prosthetic materials. Journal of biomedical materials research, 5(6), 117-141.

[3] X. Li, J. Shi, Y. Zhu, W. Shen, H. Li, J. Liang, J. Gao. 2007. A template route to the preparation of mesoporous amorphous calcium silicate with high in vitro bone-forming bioactivity. Journal of Biomedical Materials Research Part B: Applied Biomaterials, 83(2), 431-439.

[4] S.-J. Ding, M.-Y. Shie, C.-Y. Wang. 2009. Novel fast-setting calcium silicate bone cements with high bioactivity and enhanced osteogenesis in vitro. Journal of Materials Chemistry, 19(8), 1183-1190.

[5] A. Meiszterics, K. Sinkó. 2011. Study of bioactive calcium silicate ceramic systems for biomedical applications. Fifth European Conference of the International Federation for Medical and Biological Engineering, Budapest, Hungary, September 14-18.

[6] P. Taddei, A. Tinti, M.G. Gandolfi, P.L. Rossi, C. Prati. 2009. Ageing of calcium silicate cements for endodontic use in simulated body fluids: a micro-Raman study. Journal of Raman Spectroscopy, 40(12), 1858-1866.

[7] J. Wu, Y.-J. Zhu, F. Chen, X.-Y. Zhao, J. Zhao, C. Qi. 2013. Amorphous calcium silicate hydrate/block copolymer hybrid nanoparticles: synthesis and application as drug carriers. Dalton Transactions 42(19), 7032-7040.

[8] C.A. Barta, K. Sachs-Barrable, J. Jia, K.H. Thompson, K.M. Wasan, C. Orvig. 2007. Lanthanide containing compounds for therapeutic care in bone resorption disorders, Dalton Transactions (43), 5019-5030.

[9] S.V. Dorozhkin. 2015. Calcium orthophosphate bio ceramics. Ceramics International, 41(10), 13913-13966.

[10] P.S. Gomes, C. Botelho, M.A. Lopes, J.D. Santos, M.H. Fernandes. 2010. Evaluation of human osteoblastic cell response to plasma-sprayed silicon-substituted hydroxyapatite coatings over titanium substrates. Journal of Biomedical Materials Research Part B: Applied Biomaterials, 94(2), 337-346.

[11] E. Thian, J. Huang, M. Vickers, S. Best, Z. Barber, W. Bonfield. 2006. Silicon-substituted hydroxyapatite (SiHA): A novel calcium phosphate coating for biomedical applications. Journal of Materials science 41(3), 709-717.

[12] L.C. Gerber, N. Moser, N.A. Luechinger, W.J. Stark, R.N. Grass. 2012. Phosphate starvation as an antimicrobial strategy: the controllable toxicity of lanthanum oxide nanoparticles. Chemical Communications 48(32), 3869-3871.

[13] E.E. Quist, B.D. Roufogalis. 1975. Determination of the stoichiometry of the calcium pump in human erythrocytes using lanthanum as a selective inhibitor. FEBS letters, 50(2), 135-139.

[14] Y. Liu, Q. Zhang, N. Zhou, J. Tan, J. Ashley, W. Wang, F. Wu, J. Shen, M. Zhang. 2020. Study on a Novel Poly (vinyl alcohol)/Graphene Oxide-Citicoline Sodium-Lanthanum Wound Dressing: Biocompatibility, Bioactivity, Antimicrobial Activity, and Wound Healing Effect. Chemical Engineering Journal, 125059.

[15] M. Jaiswal, V. Koul, A.K. Dinda. 2016. In vitro and in vivo investigational studies of a nanocomposite-hydrogel-based dressing with a silver-coated chitosan wafer for full-thickness skin wounds. Journal of Applied Polymer Science, 133(21).

[16] Qu, X. Zhao, Y. Liang, T. Zhang, P.X. Ma, B. Guo. 2018. Antibacterial adhesive injectable hydrogels with rapid self-healing, extensibility and compressibility as wound dressing for joints skin wound healing. Biomaterials, 183, 185-199.

[17] D.B. Mathi, D. Gopi, L. Kavitha. 2020. Implication of lanthanum substituted hydroxyapatite/poly (n-methyl pyrrole) bilayer coating on titanium for orthopedic applications. Materials today: proceedings, 26, 3526-3530.

[18] M. Akram, A.Z. Alshemary, Y.-F. Goh, W.A.W. Ibrahim, H.O. Lintang, R. Hussain. 2015. Continuous microwave flow synthesis of mesoporous hydroxyapatite. Materials Science and Engineering: C, 56, 356-362.

[19] M. Akram, R. Hussain, F.K. Butt, M. Latif. 2019. Study of the effect of microwave holding time on the physicochemical properties of titanium oxide. Materials Research Express, 6(8), 085041.

[20] R.E. Ngida, M. Zawrah, R. Khattab, E. Heikal. 2019. Hydrothermal synthesis, sintering and characterization of nano La-manganite perovskite doped with Ca or Sr. Ceramics International, 45(4), 4894-4901.

[21] R. Ghosh, R. Sarkar, S. Paul. 2016. Development of machinable hydroxyapatite-lanthanum phosphate composite for biomedical applications. Materials & Design, 106, 161-169.

[22] B. Nasiri-Tabrizi, P. Honarmandi, R. Ebrahimi-Kahrizsangi, P. Honarmandi. 2009. Synthesis of nanosize single-crystal hydroxyapatite via mechanochemical method. Materials Letters, 63(5), 543-546.

[23] F. Shirazi, M. Mehrali, A. Oshkour, H. Metselaar, N. Kadri, N.A. Osman. 2014. Mechanical and physical properties of calcium silicate/alumina composite for biomedical engineering applications. Journal of the mechanical behavior of biomedical materials, 30, 168-175.

[24] G. de Souza Balbinot, V.C.B. Leitune, J.S. Nunes, F. Visioli, F.M. Collares. 2020. Synthesis of sol–gel derived calcium silicate particles and development of a bioactive endodontic cement. Dental Materials, 36(1), 135-144.

[25] M. Mabrouk, S.A. ElShebiney, S.H. Kenawy, G.T. El-Bassyouni, E.M. Hamzawy. 2019. Novel, cost-effective, Cu-doped calcium silicate nanoparticles for bone fracture intervention: Inherent bioactivity and in vivo performance. Journal of Biomedical Materials Research Part B: Applied Biomaterials, 107(2), 388-399.

[26] Y. Arslan, E. Kendüzler, V.T. Adigüzel, F. Tomul. 2019. The Effect of Synthesis Conditions on Calcium Silicate Bioceramic Materials. Journal of Natural & Applied Sciences, 23(3).

[27] T. Kozawa, K. Yanagisawa, A. Yoshida, A. Onda, Y. Suzuki. 2013. Preparation of β-CaSiO$_3$ powder by water vapor-assisted solid-state reaction. Journal of the Ceramic Society of Japan, 121(1409),103-105.

[28] K.B. Kale, R.Y. Raskar, V.H. Rane, A.G. Gaikwad. 2012. Preparation and Characterization of Calcium Silicate for CO$_2$ Sorption. Adsorption Science & Technology, 30(10), 817-830.

[29] W. Widayat, T. Darmawan, H. Hadiyanto, R.A. Rosyid. 2017. Preparation of Heterogeneous CaO Catalysts for Biodiesel Production. Journal of Physics: Conference Series, 012018.

[30] R. Atchudan, N. Lone, J. Joo. 2018. Preparation of CaCO$_3$ and CaO Nanoparticles via Solid-State Conversion of Calcium Oleate Precursor. Journal of nanoscience and nanotechnology, 18(3), 1958-1964.

[31] C.T. Yamashita, J. So, M. Fuji. 2016. Synthesis and characterization of CaO@ SiO$_2$ nanoparticle for chemical thermal storage. Journal of the Ceramic Society of Japan, 124(1), 55-59.

[32] P.E. Sanchez-Jimenez, L.A. Perez-Maqueda, J. Valverde. 2014. Nanosilica supported CaO: a regenerable and mechanically hard CO_2 sorbent at Ca-looping conditions. Applied energy, 118, 92-99.

[33] F. Puertas, F. Trivino. 1985. Examinations by infra-red spectroscopy for the polymorphs of dicalcium silicate. Cement and Concrete Research, 15(1), 127-133.

[34] A. Bouregba, A. Diouri. 2016. Potential formation of hydroxyapatite in total blood and dicalcium silicate elaborated from shell and glass powders. Materials Letters, 183, 405-407.

[35] R. Choudhary, S. Koppala, S. Swamiappan. 2015. Bioactivity studies of calcium magnesium silicate prepared from eggshell waste by sol–gel combustion synthesis. Journal of Asian Ceramic Societies, 3(2), 173-177.

[36] A.A. Pathan, K.R. Desai, C. Bhasin. 2017. Synthesis of La_2O_3 nanoparticles using glutaric acid and propylene glycol for future CMOS applications. International journal of Nanomaterials and Chemistry, 3, 21-25.

[37] A. Z. Alshemary, Yi-Fan Goh, M. Akram, M. R. Abdul Kadir, and R. Hussain. 2015. Barium and fluorine doped synthetic hydroxyapatite: characterization and in-vitro bioactivity analysis." Science of Advanced Materials 7, no. 2 249-257.

[38] A. Bernhardt, R. Dittrich, A. Lode, F. Despang and M. Gelinsky. 2013. Nanocrystalline spherical hydroxyapatite granules for bone repair: in vitro evaluation with osteoblast-like cells and osteoclasts." Journal of Materials Science: Materials in Medicine 24, no. 7, 1755-1766.

[39] S. Jadalannagari, K. Deshmukh, A.K. Verma, R.V. Kowshik, S.R. Meenal Ramanan. 2014. Lanthanum-doped hydroxyapatite nanoparticles as biocompatible fluorescent probes for cellular internalization and biolabeling. Science of Advanced Materials, 6(2), 312-319.

[40] Y. Bozkurt, S. Pazarlioglu, H. Gokce, I. Gurler, S. Salman. 2015. Hydroxyapatite lanthanum oxide composites. Acta Physica Polonica A, 127(4), 1407-1409.

[41] L.-j. Chen, C. Tian, C. Jun, B.-l. Liu, C.-s. Shao, K.-c. Zhou, D. Zhang. 2018. Effect of Tb/Mg doping on composition and physical properties of hydroxyapatite nanoparticles for gene vector application. Transactions of Nonferrous Metals Society of China, 28(1), 125-136.